PHILOSOPHICAL TRANSACTIONS OF THE ROYAL SOCIETY B BIOLOGICAL SCIENCES

Anguilliform Body Dynamics: Modelling the Interaction between Muscle Activation and Body Curvature

Graham Bowtell and Thelma L. Williams

Phil. Trans. R. Soc. Lond. B 1991 **334**, 385-390
doi: 10.1098/rstb.1991.0123

Anguilliform body dynamics: modelling the interaction between muscle activation and body curvature

GRAHAM BOWTELL AND THELMA L. WILLIAMS

Mathematics Department, City University, Northampton Square, London EC1V 0HB, U.K. and Physiology Department, St George's Hospital Medical School, University of London, London SW17 0RE, U.K.

SUMMARY

A simple two-dimensional rod and pivot model is proposed for the mechanical structure of the lamprey, each pivot being controlled by a muscle segment attached via perpendicular extensions to the two rods. The elastic and viscous properties of the body tissues (including muscle) are described as linear functions of the relative displacement and angular velocity of the rods at each pivot. The contractile properties of the muscle are introduced as time-dependent forcing torques at the pivots, which are generated by a travelling wave of activation. The angles between the rods at each pivot are used as adapted coordinates, and the equations of motion are linearized by assuming low curvature dynamics, corresponding to slow swimming speeds. Investigation of these equations with varying viscous and elastic parameters leads to a reconstruction of a lamprey viewed in motion on a smooth flat surface out of water. The most striking feature is of an apparently standing wave motion, which is indeed observed in the real animal but which on careful examination in the model corresponds to a travelling wave of varying amplitude.

1. INTRODUCTION

Anguilliform (eel-like) fish swim by passing a wave of lateral curvature from head to tail, thereby developing a thrust that pushes the animal forward (Breder 1926; Gray 1933). The patterns of muscle activation which give rise to this movement are generated by the central nervous system (for references see Grillner *et al.* (1987)). During steady-state swimming the pattern consists of bursts of ventral root activity which alternate between the left and right sides at each segmental level, with a rostral–caudal delay between neighbouring segments along each side. Thus the pattern is that of a travelling wave of muscle activation. Faster swimming is accomplished by a decrease in the duration of the activity cycle, accompanied by a proportional change in the various time delays within the pattern. This proportional change results in an intersegmental delay that is a constant fraction of the cycle, for all swimming speeds. In the lamprey it has a value of approximately 1% of a cycle per segment (Wallen & Williams 1984). The lamprey consists of approximately 100 segments, so at any swimming speed the 'wave length' of the activation pattern is approximately one body length.

The arrangement of muscle fibres and connective tissue elements within the body of a fish is such that activation of the contractile filaments within one myosegment (on the left or right side) produces tension tending to develop a local curvature concave to the active side (Gray 1933; Alexander 1969; Wainwright 1983). Development of this curvature is opposed by the inertial, viscous and elastic properties of the spinal cord or notochord, the skin, the muscle itself, and the surrounding water. The interaction of all these elements in response to the travelling wave of muscle activation results in the observed time-dependent variations in the shape of the animal, namely, the mechanical wave of curvature travelling from head to tail.

The speed of travel of the mechanical wave is slower than that of the wave of activation (Grillner & Kashin 1976), so that the relative timing of muscle activation and local curvature changes along the body length (Williams *et al.* 1989). In the hope of gaining insight into the mechanisms responsible for the observed relative timing, we have investigated the behaviour of a two-dimensional model of the body of an anguilliform fish, containing both elastic and viscous elements, and subjected to a time-varying longitudinal force generated by muscle activity within each segment. We have not here considered the effects of a surrounding fluid (Carling & Williams 1991); thus any predicted motion is that of a free animal on a smooth horizontal surface. A preliminary report of these results has appeared (Williams & Bowtell 1990).

2. MECHANICAL MODEL

The body of the animal is assumed to consist of a series of tissue segments attached via perpendicular extensions to a set of smoothly linked rods, constrained to lie in a horizontal plane (figure 1). Because the mass of the animal is symmetric about the axial midline, we assume that all the mass is distributed along this line. The swimming muscles in the real animal are

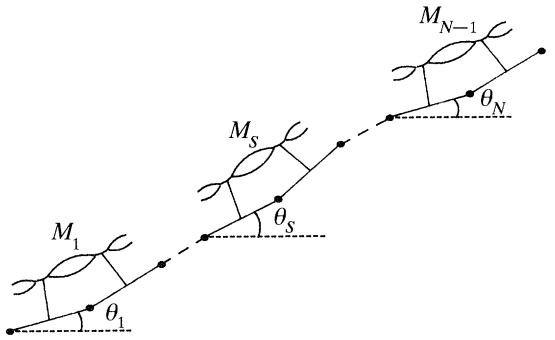

Figure 1. Representation of anguilliform body. N pivoted rods of length l with a mass m at each pivot and at both ends are controlled by muscle segments. The fixed ends of the (s)th muscle unit are a distance w from the (s)th and $(s+1)$th rod. The (s)th rod makes an angle θ_s with a line drawn through the (s)th pivot, parallel to the x-axis.

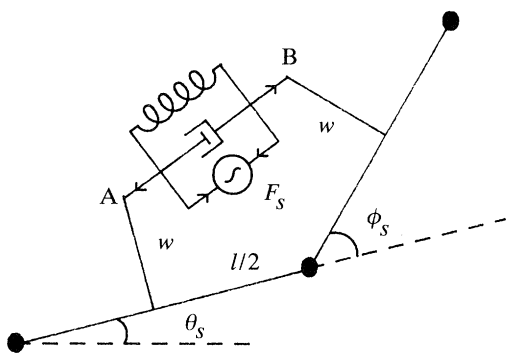

Figure 2. The (s)th tissue segment M_s consists of a spring (stiffness μ_s), a dashpot (damping coefficient γ_s) and a power source producing contractile tension $F_s(t)$, taken as positive in the direction indicated by arrows. Total thrust developed by the unit is given by the sum of the contributions of the three parallel components, and is positive in the direction shown by arrows along AB.

symmetric about the midline, and activation of muscle on the left and right sides of the body at a given segment will produce turning couples of opposite sign at the corresponding pivot. We have therefore simplified the muscle component in the model to a single-sided element which is capable of producing both positive and negative contractile force (corresponding to the algebraic sum of the force produced by muscle on both sides of the midline). Each segment of the animal is considered to contain a stiffness element modelled by a linear spring, a damping element modelled by a linear velocity-dependent dashpot, and a power unit capable of producing time-varying tension and thrust (figure 2). The elastic and damping elements model the contributions to stiffness and viscosity of all the body tissues, including the muscle itself as well as the skin, connective tissue, and spinal column or notochord.

With reference to figure 2 and applying simple geometry

$$\mathrm{AB} = l\cos(\phi_s/2) - 2w\sin(\phi_s/2). \quad (1)$$

The total thrust tending to increase the length AB is given by

$$G_s = -\mu_s(x_s/l) - \gamma_s(\dot{x}_s/l) - F_s(t), \quad (2)$$

where μ_s and γ_s are respectively the stiffness and damping coefficients of the (s)th segment, $F_s(t)$ the force generated within the contractile elements of the muscle in that segment and x_s/l the extension per unit length which, from the expression for AB, is given by

$$x_s/l = \{[\cos(\phi_s/2) - 1] - 2(w/l)\sin(\phi_s/2)\}. \quad (3)$$

For a fuller understanding of the signs in equation (2) it is worth noting that ϕ_s and x_s are of opposite signs except when $\phi_s = x_s = 0$.

3. EQUATIONS OF MOTION

To derive the equations of motion we adopt a standard Lagrangian approach for a non-conservative system, using a kinetic energy term and generalized forces (see, for example, Goldstein (1950) or Woodhouse (1987)). We use the adapted coordinates $\theta_1, \theta_2, \ldots, \theta_N$, representing the angles made by each of the N rods with the positive x-axis, and the position (x_0, y_0) of the head (see figure 1). The positions of the masses at each of the pivots and the tail point are given, for equal segments of length l, by:

$$(x_k, y_k) = (x_0, y_0) + l\left(\sum_{i=1}^{k}\cos\theta_i, \quad \sum_{i=1}^{k}\sin\theta_i\right), \quad k = 1, \ldots, N, \quad (4)$$

and the velocity v_k of the kth mass by

$$\underline{v}_k = (\dot{x}_0, \dot{y}_0) + l\left(-\sum_{i=1}^{k}\dot{\theta}_i\sin\theta_i, \quad \sum_{i=1}^{k}\dot{\theta}_i\cos\theta_i\right), \quad k = 1, \ldots, N. \quad (5)$$

The total kinetic energy K for the $N+1$ masses m is given by

$$K = \frac{m}{2}\left((\dot{x}_0^2 + \dot{y}_0^2) + \sum_{k=1}^{N}\underline{v}_k\cdot\underline{v}_k\right). \quad (6)$$

After substitution for $\underline{v}_k$,

$$K = \frac{m}{2}\Bigg((N+1)(\dot{x}_0^2 + \dot{y}_0^2) + \sum_{i=1}^{N}(N-i+1)\,l^2\dot{\theta}_i^2 + 2\sum_{k=2}^{N}\sum_{i=1}^{k-1}(N-k+1)\,\dot{\theta}_i\dot{\theta}_k\,l^2\cos(\theta_i-\theta_k) - 2l\dot{x}_0\sum_{i=1}^{N}(N-i+1)\,\dot{\theta}_i\sin\theta_i + 2l\dot{y}_0\sum_{i=1}^{N}(N-i+1)\,\dot{\theta}_i\cos\theta_i\Bigg). \quad (7)$$

The equations of motion with respect to the angular coordinates are given by

$$\frac{\mathrm{d}}{\mathrm{d}t}\left(\frac{\partial K}{\partial\dot{\theta}_s}\right) - \frac{\partial K}{\partial\theta_s} = G_{\theta_s}, \quad s = 1, \ldots, N, \quad (8)$$

where G_{θ_s} is the generalized force corresponding to the generalized coordinate θ_s.

Combining (7) and (8)

$$l^2m\Bigg((N-s+1)\sum_{i=1}^{s}\ddot{\theta}_i\cos(\theta_i-\theta_s)+\sum_{i=s+1}^{N+1}(N-i+1)\,\ddot{\theta}_i\cos(\theta_s-\theta_i)+\sum_{i=s+1}^{N+1}(N-i+1)\,\dot{\theta}_i^2\sin(\theta_s-\theta_i)-(N-s+1)\sum_{i=1}^{s}\dot{\theta}_i^2\sin(\theta_i-\theta_s)\Bigg)+ml(N-s+1)\,(-\ddot{x}_0\sin\theta_s+\ddot{y}_0\cos\theta_s)=G_{\theta_s},\quad s=1,\ldots,N. \tag{9}$$

The variable θ_{N+1} occurring in the above expression is introduced to add symmetry to the expression and does not correspond to any physical quantity: its coefficient is always zero.

Because zero work is done by the system under small variations of the head position coordinates x_0 and y_0, and because there are no external forces on the system, the corresponding generalized forces are zero.

The equations of motion thus lead to the following expressions for the head position:

$$x_0=\frac{lN}{2}-\frac{l}{N+1}\sum_{i=1}^{N}(N-i+1)\cos\theta_i \tag{10}$$

$$y_0=-\frac{l}{N+1}\sum_{i=1}^{N}(N-i+1)\sin\theta_i. \tag{11}$$

These equations are derived under the assumptions that initially all the coordinates and their first derivatives are zero, corresponding physically to a stationary straight creature lying along the positive x-axis with its head at the origin. As expected, since there are no external forces on the system, these equations lead to the centre of mass being fixed at the initial midpoint of the body, namely $(Nl/2, 0)$.

4. GENERALIZED FORCES

The generalized forces corresponding to the $N+2$ coordinates are obtained in the usual manner by considering the work done by the system under small independent changes of each of the coordinates in turn. As noted above the generalized forces corresponding to the head coordinates x_0 and y_0 are zero. To calculate the other forces, namely G_{θ_s}, we need to consider the geometry of the system and in particular that of a typical muscle element. With the exception of θ_1 and θ_N a small change of Δ_{θ_s} in θ_s only is attained by a change in the muscle segments M_{s-1} and M_s. This is clear from observing that the angle ϕ_s at the (s)th pivot, namely $\phi_s=\theta_{s+1}-\theta_s$, $s=1,\ldots,N-1$, is decreased by Δ_{θ_s} and the corresponding angle ϕ_{s-1} at the $(s-1)$th pivot is increased by Δ_{θ_s}. No other pivotal angles are affected by this change in θ_s. Thus for positive Δ_{θ_s} the unit in the (s)th segment is extended and in the $(s-1)$th segment shortened.

Thus the total work done, to first order in Δ_{θ_s}, by the resultant thrusts G_s and G_{s-1} in the (s)th and $(s-1)$th segments due to the change Δ_{θ_s} in θ_s is given by

$$\{l/2\,[G_s\sin(\phi_s/2)-G_{s-1}\sin(\phi_{s-1}/2)]+w[G_s\cos(\phi_s/2)-G_{s-1}\cos(\phi_{s-1}/2)]\}\,\Delta_{\theta_s}. \tag{12}$$

The generalized force G_{θ_s} is therefore given by the coefficient of Δ_{θ_s} in the above expression and if we set the non-physical constants G_0 and G_N to zero it is valid for $s=1,\ldots,N$.

The forcing function $F_s(t)$ in equation (2) represents the timecourse of activation of the contractile protein filaments. EMG recordings from swimming animals show that each burst of ventral root activity occupies approximately 40% of a cycle, with strict left–right alternation (Wallen & Williams 1984). Because activity on the contralateral side is modelled as negative values, this pattern can be approximated by a sine wave, or by a square wave with a mean value of zero. We have also allowed attenuation at the rostral and caudal ends. The following forcing functions have been investigated.

Square wave: the function

$$F_s(t)=F(kx-\omega t),\quad \text{where}\quad x=\frac{(s-1)}{(N-2)},\quad s=1,\ldots,N-1, \tag{13}$$

with

$$F(y)=\begin{cases}0 & 0\leqslant y\leqslant 0.1\\ 1 & 0.1<y<0.5\\ 0 & 0.5\leqslant y\leqslant 0.6\\ -1 & 0.6<y<1\end{cases}$$

extended periodically beyond $[0, 1]$.

Sine wave:

$$F_s(t)=\sin(kx-\omega t),\quad \text{where}\quad x=\frac{(s-1)}{(N-2)},\quad s=1,\ldots,N-1. \tag{14}$$

Attenuated sine wave:

$$F_s(t)=\exp\left(\frac{-\beta}{x(1-x)}\right)\sin(kx-\omega t),\quad x=\frac{(s-1)}{(N-2)},\quad s=2,\ldots,N-2,\quad =0\quad s=1,N-1. \tag{15}$$

5. LINEARIZATION

We now make the obvious linearization of equation (9) assuming θ_s, $\dot{\theta}_s$ and ϕ_s are small. With the extension per unit length now given by $-w\phi_s/l$ the generalized forces are approximated by $G_{\theta_s}=w(G_s-G_{s-1})$ where G_s is given by equations (2) and (3), which in linearized form become

$$G_s=\mu_s(w/l)\,\phi_s+\gamma_s(w/l)\,\dot{\phi}_s-F_s(t),\quad s=1,\ldots,N-1. \tag{16}$$

The linearized equations of motion for the angular coordinates are given by

$$G_{\theta_s}=l^2m\Bigg\{\Bigg((N-s+1)\sum_{i=1}^{s}\ddot{\theta}_i+\sum_{i=s+1}^{N+1}(N-i+1)\,\ddot{\theta}_i-\frac{(N-s+1)}{(N+1)}\sum_{i=1}^{N}(N-i+1)\,\ddot{\theta}_i\Bigg\}\quad s=1,\ldots,N, \tag{17}$$

and the position of the head by:

$$x_0 = 0 \quad \text{and} \quad y_0 = \frac{-l}{N+1} \sum_{i=1}^{N} (N-i+1)\,\theta_i. \tag{18}$$

Introducing two other zero dummy variables G_{-1} and G_{N+1} the following manipulations lead to a set of equations for $\ddot{\theta}_s$ in terms of lower derivative terms; with the G_{θ_s} terms given by equation (17)

$$G_{\theta_s} - G_{\theta_{s+1}} = ml^2 \left\{ \sum_{i=1}^{s} \ddot{\theta}_i - \frac{1}{(N+1)} \sum_{i=1}^{N} (N-i+1)\,\ddot{\theta}_i \right\}, \quad s = 1, \ldots, N, \tag{19}$$

$$(G_{\theta_s} - G_{\theta_{s+1}}) - (G_{\theta_{s-1}} - G_{\theta_s}) = ml^2 \ddot{\theta}_s, \quad s = 1, \ldots, N. \tag{20}$$

Finally substituting for G_{θ_s} from equation (16) leads to

$$ml^2 \ddot{\theta}_s = -(G_{s+1} - 3G_2 + 3G_{s-1} - G_{s-2})\,w, \quad s = 1, \ldots, N. \tag{21}$$

It is more natural to specify the angular motion of the system by $\{\theta_1, \phi_1, \ldots, \phi_{N-1}\}$ as the spring and dashpot forces in each segment depend only on the ϕ variables, i.e. the amount of bending at each segment.

Thus from equation (21)

$$\ddot{\phi}_s = -\frac{w}{ml^2} \{G_{s+2} - 4G_{s+1} + 6G_s - 4G_{s-1} + G_{s-2}\}, \quad s = 1, \ldots, N-1. \tag{22}$$

6. NUMERICAL INVESTIGATION

The set of linearized equations was investigated numerically to predict actual observed motions. This simple linear problem lends itself to numerical solution using a fourth order Runge Kutta routine. To observe the movements induced by the forcing term a simple time lapse graphical output was constructed.

Values were chosen for k and ω in the forcing function F_s so as to produce a wave of muscle activation with a wave length of approximately one body length and a frequency of two cycles per second, a typical swimming frequency for a lamprey. The physical constants of mass and length were chosen to make the total length and total mass of the body equal to unity. Thus $m = 1/(N+1)$ and $l = 1/N$. The half-width w has been chosen by observing that the width of a typical lamprey is about 4% of its length, thus w is set equal to 0.02. In preliminary experiments, results were qualitatively similar for N greater than 10. So N was set equal to 20.

A more difficult task was the selection of the parameters of stiffness and damping, as these are not easily estimated from knowledge of the intact animal. To choose a reasonable range of values, we have considered the hypothetical behaviour of a single inactive muscle segment after being mechanically displaced by an external force. So for the single segment in figure 2, setting θ_s and F_s equal to zero corresponds to a single unforced muscle segment with one arm fixed, and is used to represent an inert tissue element at either end of the animal. We then investigated the behaviour of such a model in response to an initial displacement from the equilibrium position, and have introduced a new set of parameters (α, T). These parameters measure respectively: (i) the degree of damping (namely underdamped, overdamped or critically damped) and (ii) the response time for a single inactive tissue segment to return to its position of equilibrium when mechanically displaced by an external force. We have used a domain for each parameter which spans two orders of magnitude.

Dropping the suffices from the symbols of figure 2, the equation of motion for small displacements of this single element is given by:

$$\ddot{\phi} + \frac{w^2\gamma}{ml^3}\dot{\phi} + \frac{w^2\mu}{ml^3}\phi = 0. \tag{23}$$

Setting $\alpha = 4\mu l^3 m / w^2 \gamma^2$, equation (23) is critically damped if $\alpha = 1$, underdamped if $\alpha > 1$ and overdamped if $\alpha < 1$. It seemed reasonable to require that α should not be greater than one, as this would give rise to oscillatory behaviour in response to a small displacement of the end segments. Thus $\{0.01, 0.1, 1\}$ was chosen as the domain for α. Using equation (23), the parameter T was defined as the time required for the single segment to return to ten percent of its original displacement. A range of values from 10 ms to 1 s seemed reasonable, so the parameter space for T (in seconds) was also chosen to be $\{0.01, 0.1, 1\}$. For given values of T and α the corresponding values of the stiffness and damping parameters are easily calculated, these parameters taken to be constant for each segment of the body.

7. RESULTS

Qualitatively there was very little difference in the movement profiles obtained from the three different forcing functions, at any point in the parameter space. The results illustrated in figure 3 were obtained with the forcing function given by equation (15).

For the (T, α) parameters equal to $(1, 0.1)$, $(1, 1)$ or $(0.1, 1)$ the transient parts of the solutions were slow to die away (more than two seconds) and therefore were not considered further, as such a lengthy transient seems unrealistic. Over the rest of the parameter space, the observed movement profile was that of a travelling wave with an envelope which possesses two or three nodal points. The superposition of such profiles over one cycle are shown in figure 3*a*, *c*, *e*. For the (T, α) pair $(1, 0.01)$ the attenuation of the travelling wave profile was slight (figure 3*e*), so that the overall impression was that of a travelling wave, although the attenuation near the tail made it unlike the pattern seen in the intact swimming lamprey (figure 3*f*). For all other pairs in the parameter space, the attenuation of the travelling wave profile into two or three nodal points was so severe as to give the initial impression of a standing wave (figure 3*a*, *c*). On closer inspection, however, it can be seen that a wave of curvature travels to and through the nodes.

Having failed to obtain results that mimicked intact swimming lampreys, we decided to observe the behaviour of intact lampreys out of water, on a smooth surface. Superimposed tracings from single video

PHILOSOPHICAL TRANSACTIONS OF THE ROYAL SOCIETY B BIOLOGICAL SCIENCES

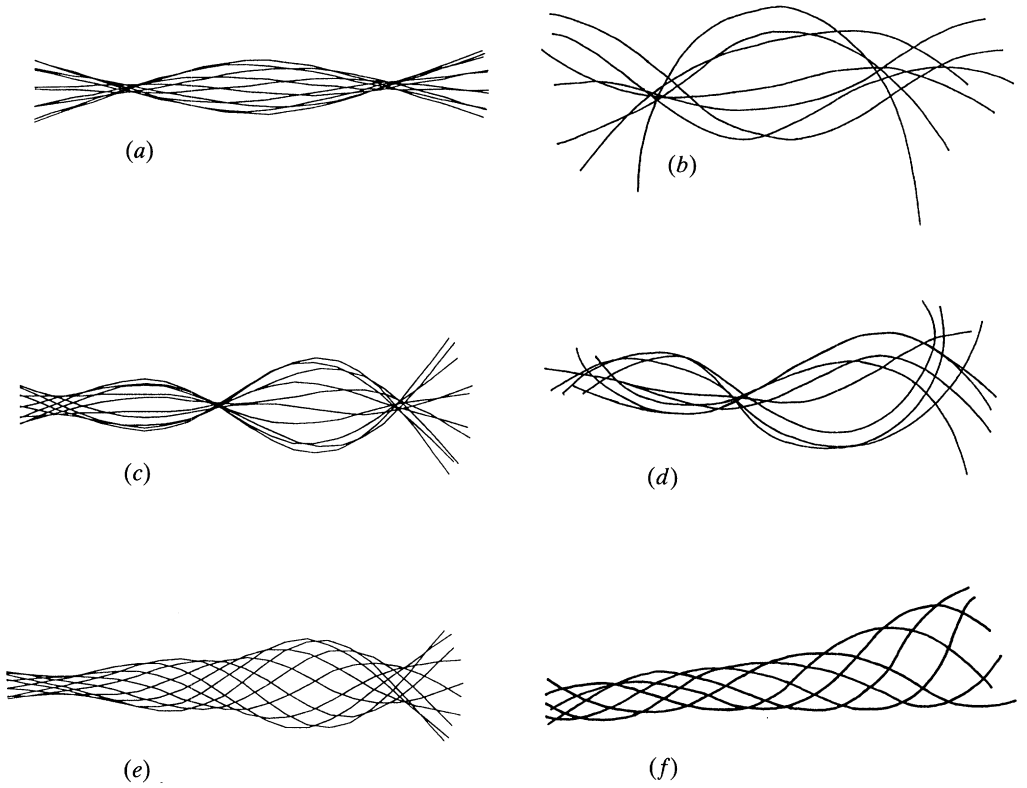

Figure 3. Comparison of calculated profiles (a, c, e) with those of intact lamprey (b, d, f). Parameters (α, T) for calculated profiles were: (a) $(1.0, 0.01)$, (c) $(0.1, 0.1)$ and (e) $(0.01, 1.0)$; (b) and (d) are traces from single frames of a video recording of an intact lamprey on a wet bench; (f) consists of superimposed traces from single frames of a cine film of an intact lamprey swimming in a swimmill (Williams *et al.* 1989).

frames are shown in figure 3*b*, *d* for two different movement sequences, for comparison with the behaviour of the model. As with the model, in any one movement sequence, the profile resembled either a standing wave with two nodes, or one with three. If, however, a thick enough layer of water was placed on the bench, the movement took on the appearance of a travelling wave, and the lamprey made forward (albeit slow) progress.

8. DISCUSSION

The similarity between the behaviour of the model over a wide parameter space and the behaviour of an intact lamprey on a smooth surface indicates that this simple linear model for the mechanical structure of the lamprey and the interaction between the muscle filaments and the surrounding tissues may be sufficient for further investigations of the control of movement in this animal. When we first began to model the lamprey body as a viscoelastic structure acted upon by a forcing function, we anticipated that the effects of the surrounding water on the movement of the animal might be incorporated within the lumped parameters of elasticity and viscosity, μ and γ (Williams 1991). Our results have made it clear, however, that even a qualitative understanding of the relative timing of activation and movement in the intact swimming animal will require fluid dynamical analysis. Such an analysis is now being undertaken (Carling & Williams 1991).

Apart from investigating the effect of the nonlinear terms in the above model there is also one important physical property of the animal that has yet to be considered. In the real animal the force generated by the contractile elements is dependent upon the muscle length and its rate of change with respect to time. This can be included in the model by extending the dependence of F_s to ϕ_s and $\dot{\phi}_s$. In addition, in the real animal there is sensory feedback to the neurally generated pattern which is dependent upon the timecourse of local curvature. This may be included in the model as a local influence on the activation frequency ω.

Although the musculature of the animal consists of a discrete number of segments a continuum limit of equation (22) would be of general value for the further investigation and approximate analytic solution of the above linearized system. Such studies are in progress. The inclusion of nonlinear terms and the other refinements mentioned above are expected to make the model more realistic for incorporation within the fluid dynamics of the swimming lamprey.

We are grateful to John Carling for helpful comments on the manuscript. This work was supported by the SERC. A preliminary report has appeared (Williams & Bowtell 1990).

REFERENCES

Alexander, R. McN. 1969 The orientation of muscle fibres in the myomeres of fishes. *J. mar. biol. Ass.* **49**, 263–290.

Breder, C. A. 1926 The locomotion of fishes. *Zoologica* **4**, 159–297.

Carling, J. & Williams, T. L. 1991 Lamprey hydrodynamics: the numerical solution of the Navier–Stokes equations. *J. mar. biol. Ass. U.K.* (Abstract.) **71**, 711.

Goldstein, H. 1950 *Classical mechanics*. London: Addison Wesley.

Gray, J. 1933 Studies in animal locomotion I. Movement of the fish with special reference to the eel. *J. exp. Biol.* **10**, 88–104.

Grillner, S. & Kashin, S. 1976 On the generation and performance of swimming in fish. In *Neural Control of Locomotion* (ed. R. M. Herman, S. Grillner, P. S. G. Stein & D. G. Stuart), pp. 181–201. New York: Plenum.

Grillner, S., Wallen, P., Dale, N., Brodin, L., Buchanan, J. & Hill, R. 1987 Transmitters, membrane properties and network circuitry in the control of locomotion in lamprey. *Trends Neurosci.* **10**, 34–41.

Wainwright, S. A. 1983 To bend a fish. In *Fish biomechanics* (ed. P. W. Webb & D. Weihs), pp. 68–91. New York: Praeger.

Wallen, P. & Williams, T. L. 1984 Fictive locomotion in the lamprey spinal cord *in vitro* compared with swimming in the intact and spinal animal. *J. Physiol.* **347**, 225–239.

Williams, T. L. 1991 The neural-mechanical link in lamprey locomotion. In *Neural and sensory mechanisms in locomotion* (ed. D. M. Armstrong & B. M. H. Bush), pp. 183–195. Manchester University Press.

Williams, T. L. & Bowtell, G. 1990 Can a lamprey swim without water? *Eur. J. Neurosci.* (Suppl.) **3**, 62. (Abstract.)

Williams, T. L., Grillner, S., Smoljaninov, V. V., Wallen, P., Kashin, S. & Rossignol, S. 1989 Locomotion in lamprey and trout: the relative timing of activation and movement. *J. exp. Biol.* **143**, 559–566.

Woodhouse, N. M. J. 1987 *Introduction to Analytical Dynamics*. Oxford Science Publications.

Received 30 May 1991; accepted 9 August 1991

PHILOSOPHICAL TRANSACTIONS OF THE ROYAL SOCIETY B BIOLOGICAL SCIENCES